
PRUNING FILTER IN FILTER

Fanxu Meng^{1,2*}, Hao Cheng^{2*}, Ke Li², Huixiang Luo², Xiaowei Guo², Guangming Lu^{1†}, Xing Sun^{2†}

¹ School of Computer Science and Technology, Harbin Institute of Technology, Shenzhen, China

² Tencent Youtu Lab, Shanghai, China

{18S151514}@stu.hit.edu.cn, luguangm@hit.edu.cn, {louischeng, tristanli, huixiangluo, scorpioguo, winfredsun}@tencent.com

ABSTRACT

Pruning has become a very powerful and effective technique to compress and accelerate modern neural networks. Existing pruning methods can be grouped into two categories: filter pruning (FP) and weight pruning (WP). FP wins at hardware compatibility but loses at the compression ratio compared with WP. To converge the strength of both methods, we propose to prune the filter in the filter. Specifically, we treat a filter $F \in \mathbb{R}^{C \times K \times K}$ as $K \times K$ stripes, *i.e.*, 1×1 filters $\in \mathbb{R}^C$, then by pruning the stripes instead of the whole filter, we can achieve finer granularity than traditional FP while being hardware friendly. We term our method as SWP (*Stripe-Wise Pruning*). SWP is implemented by introducing a novel learnable matrix called Filter Skeleton, whose values reflect the shape of each filter. As some recent work has shown that the pruned architecture is more crucial than the inherited important weights, we argue that the architecture of a single filter, *i.e.*, the shape, also matters. Through extensive experiments, we demonstrate that SWP is more effective compared to the previous FP-based methods and achieves the state-of-art pruning ratio on CIFAR-10 and ImageNet datasets without obvious accuracy drop. Code is available at [this url](#).

1 Introduction

Deep Neural Networks (DNNs) have achieved remarkable progress in many areas including speech recognition [1], computer vision [2, 3], natural language processing [4], *etc.* However, model deployment is sometimes costly due to the large number of parameters in DNNs. To relieve such a problem, numerous approaches have been proposed to compress DNNs and reduce the amount of computation. These methods can be classified into two main categories: weight pruning (WP) and filter (channel) pruning (FP).

WP is a fine-grained pruning method that prunes the individual weights, *e.g.*, whose value is nearly 0, inside the network [5, 6], resulting in a sparse network without sacrificing prediction performance. However, since the positions of non-zero weights are irregular and random, we need an extra record of the weight position, and the sparse network pruned by WP can not be presented in a structured fashion like FP due to the randomness inside the network, making WP unable to achieve acceleration on general-purpose processors. By contrast, FP-based methods [7, 8, 9] prune filters or channels within the convolution layers, thus the pruned network is still well organized in a structure fashion and can easily achieve acceleration in general processors. A standard filter pruning pipeline is as follows: 1) Train a larger model until convergence. 2) Prune the filters according to some criterions 3) Fine-tune the pruned network. [10] observes that training the pruned model with random initialization can also achieve high performance. Thus it is the network architecture, rather than trained weights that matters. In this paper, we suggest that *not only the architecture of the network but the architecture of the filter itself is also important*. [11, 12] also draw similar arguments that the filter with a larger kernel size may lead to better performance. However, the computation cost is expensive. Thus for a given input feature map, [11, 12] uses filters with different kernel sizes (*e.g.*, 1×1 , 3×3 , and 5×5) to perform convolution and concatenate all the output feature map. But the kernel size of each filter is manually set. It needs professional experience and knowledge to design an efficient network structure. We wonder *what if we can learn the optimal kernel size of each filter by pruning*. Our intuition is illustrated in Figure 1. We know that the structure of deep nets matters for learning tasks. For example, the residual net is easier to optimize and exhibits better performance than VGG. However, we find that there is another structure hidden inside the network, which we call ‘**the shape of the filters**’. From Figure

¹In the author list, * denotes that authors contribute equally; † denotes corresponding authors. The work is conducted while Fanxu Meng works as an internship at Tencent Youtu Lab.

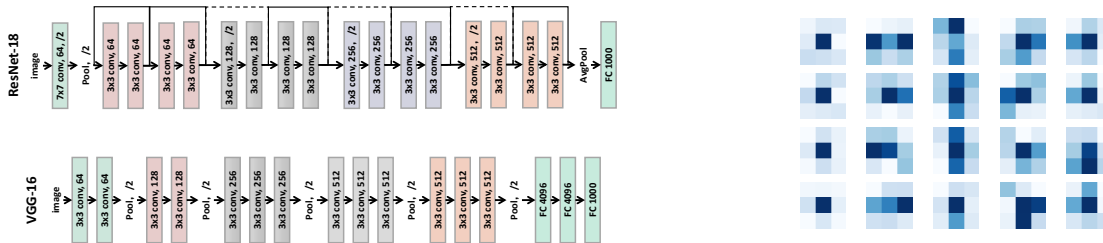


Figure 1: The left figure shows two network structures. The right figure visualizes the average l_1 norm of the filters along the channel dimension in a learned VGG16.

1, not all the stripes in a filter contribute equally [13]. Some stripes have a very low l_1 norm indicating that such stripes can be removed from the network. The shape that maintains the function of the filter while leaving the least number of stripes is named optimal shape. To capture the ‘filter shape’ alongside the filter weights, we propose ‘Filter Skeleton (FS)’ to learn this ‘shape’ property and use FS to guide efficient pruning (i.e. learn optimal shape) (See Section 3). Compared to the traditional FP-based pruning, this pruning paradigm achieves finer granularity since we operate with stripes rather than the whole filter.

Similarly, group-wise pruning, introduced in [14, 15, 16] also achieves finer granularity than filter/channel pruning, which removes the weights located in the same position among all the filters in a certain layer. However, group-wise pruning breaks the independent assumption on the filters. For example, the invalid positions of weights in each filter may be different. By regularizing the network using group-wise pruning, the network may lose representation ability under a large pruning ratio (see Section 4.2). In this paper, we also offer a comparison to group-wise pruning in the experiment. In contrast, SWP keeps each filter independent with each other which does not break the independent assumption among the filters. Throughout the experiments, SWP achieves a higher pruning ratio compared to the filter-wise, channel-wise, and group-wise pruning methods. We summarize our main contributions below:

- We propose a new pruning paradigm called SWP. SWP achieves a finer granular than traditional filter pruning and the pruned network can still be inferred efficiently.
- We introduce Filter Skeleton (FS) to efficiently learn the shape of each filter and deeply analyze the working mechanism of FS. Using FS, we achieve the state-of-art pruning ratio on CIFAR-10 and ImageNet datasets without obvious accuracy drop.

2 Related Work

Weight pruning: Weight pruning (WP) dates back to optimal brain damage and optimal brain surgeon [17, 18], which prune weights based on the Hessian of the loss function. [5] prunes the network weights based on the l_1 norm criterion and retrain the network to restore the performance and this technique can be incorporated into the deep compression pipeline through pruning, quantization, and Huffman coding [6]. [19] reduces the network complexity by making on-the-fly connection pruning, which incorporates connection splicing into the whole process to avoid incorrect pruning and make it as continual network maintenance. [20] removes connections at each DNN layer by solving a convex optimization program. This program seeks a sparse set of weights at each layer that keeps the layer inputs and outputs consistent with the originally trained model. [21] proposes a frequency-domain dynamic pruning scheme to exploit the spatial correlations on CNN. The frequency-domain coefficients are pruned dynamically in each iteration and different frequency bands are pruned discriminatively, given their different importance on accuracy. [22] divides each stripe into multiple groups, and prune weights in each group. However, one drawback of these unstructured pruning methods is that the resulting weight matrices are sparse, which cannot lead to compression and speedup without dedicated hardware/libraries [23].

Filter/Channel Pruning: Filter/Channel Pruning (FP) prunes at the level of filter, channel, or even layer. Since the original convolution structure is still preserved, no dedicated hardware/libraries are required to realize the benefits. Similar to weight pruning [5], [7] also adopts l_1 norm criterion that prunes unimportant filters. Instead of pruning filters, [8] proposed to prune channels through LASSO regression-based channel selection and least square reconstruction. [9] optimizes the scaling factor γ in the BN layer as a channel selection indicator to decide which channel is unimportant

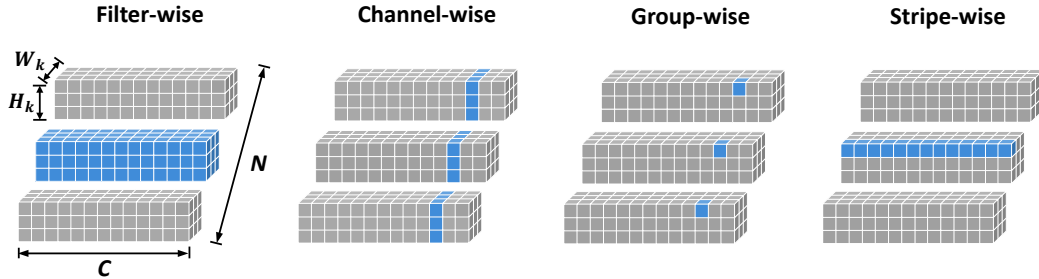


Figure 2: The visualization of different types of pruning.

Table 1: Test accuracy of each network that only learns the ‘shape’ of the filters.

Dataset	Backbone	Test accuracy
CIFAR-10	VGG16	79.83
	ResNet56	83.82
	MobileNetV2	83.52

and can be removed. [24] introduces ThiNet that formally establish filter pruning as an optimization problem, and reveal that we need to prune filters based on statistics information computed from its next layer, not the current layer. Similarly, [25] optimizes the reconstruction error of the final response layer and propagates an ‘importance score’ for each channel. [26] first proposes that utilize AutoML for Model Compression which leverages reinforcement learning to provide the model compression policy. [27] proposes an effective structured pruning approach that jointly prunes filters as well as other structures in an end-to-end manner. Specifically, the authors introduce a soft mask to scale the output of these structures by defining a new objective function with sparsity regularization to align the output of the baseline and network with this mask. [28] introduces a budgeted regularized pruning framework for deep CNNs that naturally fit into traditional neural network training. The framework consists of a learnable masking layer, a novel budget-aware objective function, and the use of knowledge distillation. [29] proposes a global filter pruning algorithm called Gate Decorator, which transforms a vanilla CNN module by multiplying its output by the channel-wise scaling factors, i.e. gate, and achieves state-of-art results on CIFAR dataset. [30, 10] deeply analyze how initialization affects pruning through extensive experimental results.

Group-wise Pruning: [14, 15] introduces group-wise pruning, that learns a structured sparsity in neural networks using group lasso regularization. The group-wise pruning can still be efficiently processed using ‘im2col’ implementation as filter-wise and channel-wise pruning. [31] further explores a complete range of pruning granularity and evaluate how it affects the prediction accuracy. [16] improves the group-wise pruning by proposing a dynamic regularization method. However, group-wise pruning removes the weights located in the same position among all the filters in a certain layer. Since invalid positions of each filter may be different, group-wise pruning may cause the network to lose valid information. In a contrast, our approach keeps each filter independent with each other, thus can lead to a more efficient network structure. Different types of pruning are illustrated in Figure 2.

Mask in Pruning: Using a (soft) mask to represent the importance of component in network has been thoroughly studied in the work of pruning [32, 33, 34, 35, 27, 36, 37, 9, 8]. However, most work design the masks in terms of the filter or channels, few works pay attention to stripes. Also, Filter Skeleton (FS) is not just a mask, we consider each filter has two properties: weight and shape. FS is to learn the ‘shape’ property. From Section 3.1 in the paper, the network still has a good performance by only learning the ‘shape’ of the filters, keeping the filter weight randomly initialized.

3 The proposed Method

3.1 Filter Skeleton (FS)

FS is introduced to learn another important property of filters alongside their weight: *shape*, which is a matrix related to the stripes of the filter. Suppose the l -th convolutional layer’s weight W^l is of size $\mathbb{R}^{N \times C \times K \times K}$, where N is the

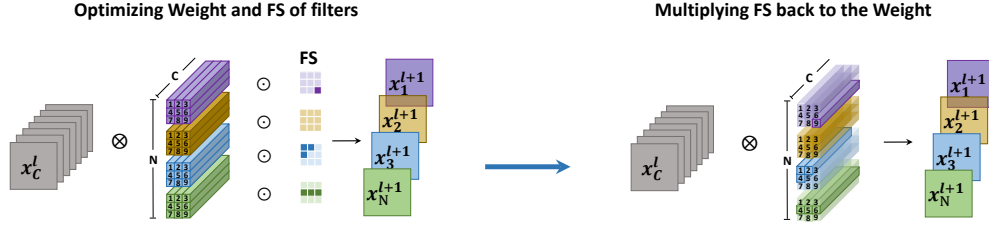


Figure 3: Training and inference with Filter Skeleton (FS).

number of the filters, C is the channel dimension and K is the kernel size. Then the size of FS in this layer is $\mathbb{R}^{N \times K \times K}$. *I.e.*, each value in FS corresponds to a strip in the filter. FS in each layer is firstly initialized with all-one matrix. During training, We multiply the filters' weights with FS. Mathematically, the loss is represented by:

$$L = \sum_{(x,y)} \text{loss}(f(x, W \odot I), y) \quad (1)$$

, where I represents the FS, \odot denotes dot product. With I , the forward process is:

$$X_{n,h,w}^{l+1} = \sum_c \sum_i \sum_j I_{n,i,j}^l \times W_{n,c,i,j}^l \times X_{n,h+i-\frac{K+1}{2},w+j-\frac{K+1}{2}}^l \quad (2)$$

. The gradient with regard to W and I is:

$$\text{grad}(W_{n,c,i,j}^l) = I_{n,i,j}^l \times \sum_h \sum_w \frac{\partial L}{\partial X_{n,h,w}^{l+1}} \times X_{c,h+i-\frac{K+1}{2},w+j-\frac{K+1}{2}}^l \quad (3)$$

$$\text{grad}(I_{n,i,j}^l) = \sum_c (W_{n,c,i,j}^l \times \sum_h \sum_w \frac{\partial L}{\partial X_{n,h,w}^{l+1}} \times X_{c,h+i-\frac{K+1}{2},w+j-\frac{K+1}{2}}^l) \quad (4)$$

, where M_H, M_W represent the height and width of the feature map respectively. $X_{c,p,q}^l = 0$ when $p < 1$ or $p > M_H$ or $q < 1$ or $q > M_W$ (this corresponds to the padding and shifting[38, 39] procedures).

From (1), the filter weights and FS are jointly optimized during training. After training, we merge I onto the filter weights W (*i.e.*, $W \leftarrow W \odot I$), and only use W during evaluating. Thus no additional cost is brought to the network when applying inference. The whole process is illustrated in Figure 3. To further show the importance of the 'shape' property, we conduct an experiment where the filters' weights are fixed, only FS can be optimized during training. The results are shown on Table 1. It can be seen that without updating the filters' weights, the network still gets decent results. We also find that with Filter Skeleton, the weights of the network become more stable. Figure 4 displays the distribution of the weights of the baseline network and network trained by Filter Skeleton (FS). It can be seen that the weights trained by FS are sparse and smooth, which have a low variance to input images, leading to stable outputs. Thus the network is robust to the variation of the input data or features.

3.2 Stripe-wise pruning with FS

From Figure 1, not all the stripes contribute equally in the network. To build a compact and highly pruned network, the Filter Skeleton (FS) needs to be sparse. *I.e.*, when some values in FS is close to 0, the corresponding stripes can be pruned. Therefore, when training the network with FS, we impose regularization on FS to make it sparse:

$$L = \sum_{(x,y)} \text{loss}(f(x, W \odot I), y) + \alpha g(I) \quad (5)$$

, where α controls the magnitude of regularization, $g(I)$ indicates l_1 norm penalty on I , which is commonly used in many pruning approaches [7, 8, 9]. Specifically, $g(I)$ is written as:

$$g(I) = \sum_{l=1}^L g(I^l) = \sum_{l=1}^L \left(\sum_{n=1}^N \sum_{i=1}^K \sum_{j=1}^K |I_{n,i,j}^l| \right). \quad (6)$$

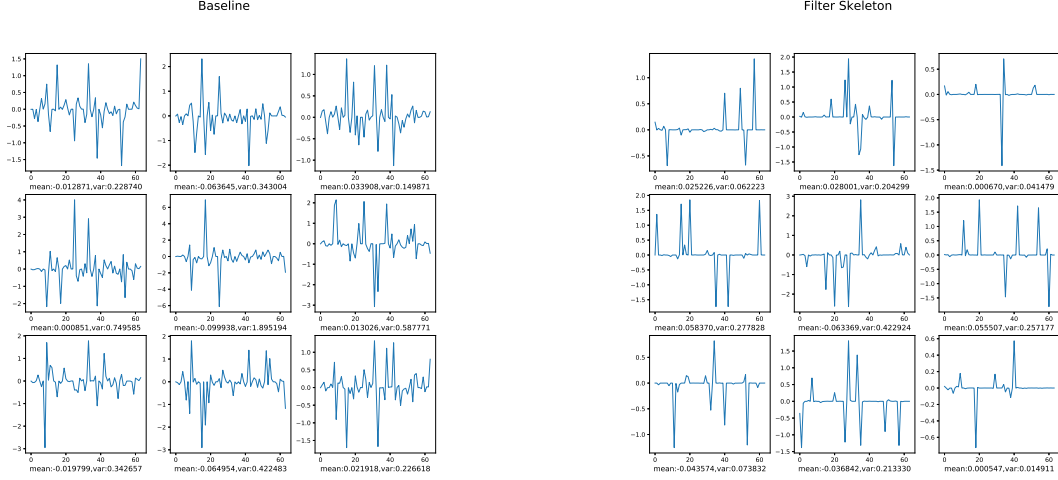


Figure 4: This left and the right figure shows the distribution of the weights of baseline and FS on the first convolution layer, respectively. In this layer, each filter has 9 strips. Each mini-figure shows the l_1 norm of the stripes located in the same position of all the filters. The mean and std are also reported.

From (5), FS implicitly learns the optimal shape of each filter. In Section 4.4, we visualize the shape of filters to further show this phenomenon. To lead efficient pruning, we set a threshold δ , the stripes whose corresponding values in FS are smaller than δ will not be updated during training and can be pruned afterwards. It is worth noticing that when performing inference on the pruned network, we can not directly use the filter as a whole to perform convolution on the input feature map since the filter is broken. Instead, we need to use each stripe independently to perform convolution and sum the feature map produced by each stripe, as shown in Figure 5. Mathematically, the convolution process in SWP is written as:

$$\begin{aligned}
 X_{n,h,w}^{l+1} &= \sum_c \sum_i \sum_j W_{n,c,i,j}^l \times X_{n,h-i+\frac{K+1}{2},w-j+\frac{K+1}{2}}^l \quad \text{standard convolution} \\
 &= \sum_i \sum_j \left(\sum_c W_{n,c,i,j}^l \times X_{n,h-i+\frac{K+1}{2},w-j+\frac{K+1}{2}}^l \right) \quad \text{stripe wise convolution}
 \end{aligned} \tag{7}$$

, where $X_{n,h,w}^{l+1}$ is one point of the feature map in the $l+1$ -th layer. From (7), SWP only modifies the calculation order in the conventional convolution process, thus no additional operations (Flops) are added to the network. It is worth noting that, since each stripe has its own position in the filter. SWP needs to record the indexes of all the stripes. However, it costs little compared to the whole network parameters. Suppose the l -th convolutional layer's weight W^l is of size $\mathbb{R}^{N \times C \times K \times K}$. For SWP, we need to record $N \times K \times K$ indexes. Compared to the individual weight pruning which records $N \times C \times K \times K$ indexes, we reduce the weight pruning's indexes by C times. Also, we do not need to record the indexes of the filter if all the stripes in such filter are removed from the network, and SWP degenerates to conventional filter-wise pruning. For a fair comparison with traditional FP-based methods, we add the number of indexes when calculating the number of network parameters.

There is two advantage of SWP compared to the traditional FP-based pruning:

- Suppose the kernel size is $K \times K$, then SWP achieves $K^2 \times$ finer granularity than traditional FP-based pruning, which leads to a higher pruning ratio.
- For certain datasets, *e.g.*, CIFAR-10, the network pruned by SWP keeps high performance even without a fine-tuning process. This separates SWP from many other FP-based pruning methods that require multiple fine-tuning procedures. The reason is that FS learns an optimal shape for each filter. By pruning unimportant stripes, the filter does not lose much useful information. In contrast, FP pruning directly removes filters which may damage the information learned by the network.

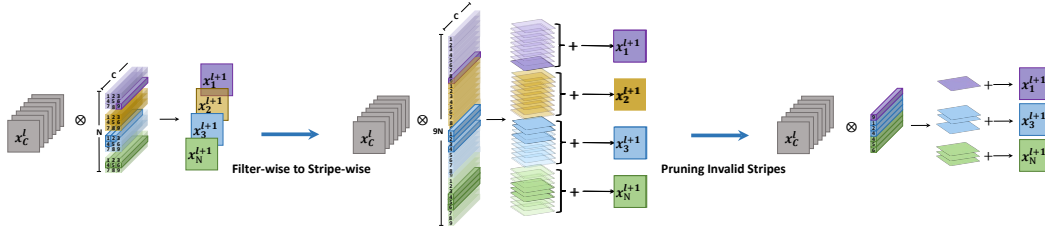


Figure 5: Pruning process in SWP.

4 Experiments

This section arranges as follows: In Section 4.1, we introduce the implementation details in the paper; in Section 4.2, we compare SWP with group-wise pruning; in Section 4.3, we show SWP achieves state-of-art pruning ratio on CIFAR-10 and ImageNet datasets compared to filter-wise, channel-wise or shape-wise pruning; in Section 4.4, we visualize the pruned filters; in Section 4.5, we perform ablation studies to study how hyper-parameters influence SWP.

4.1 Implementation Details

Datasets and Models: CIFAR-10 [40] and ImageNet [41] are two popular datasets and are adopted in our experiments. CIFAR-10 dataset contains 50K training images and 10K test images for 10 classes. ImageNet contains 1.28 million training images and 50K test images for 1000 classes. On CIFAR-10, we evaluated our method on two popular network structures: VGG16 [42], ResNet56 [43]. On ImageNet dataset, we adopt ResNet18.

Baseline Setting: Our baseline setting is consistent with [9]. For CIFAR-10, the model was trained for 160 epochs with a batch size of 64. The initial learning rate is set to 0.1 and divide it by 10 at the epoch 80 and 120. The simple data augmentation (random crop and random horizontal flip) is used for training images. For ImageNet, we follow the official PyTorch implementation¹ that train the model for 90 epochs with a batch size of 256. The initial learning rate is set to 0.1 and divide it by 10 every 30 epochs. Images are resized to 256×256 , then randomly crop a 224×224 area from the original image for training. The testing is on the center crop of 224×224 pixels.

SWP setting: The basic hyper-parameters setting is consistent with the baseline. α is set to $1e-5$ in (5) and the threshold δ is set to 0.05. For CIFAR-10, we do not fine-tune the network after stripe selection. For ImageNet, we perform a one-time fine-tuning after pruning.

4.2 Group-wise pruning vs stripe-wise pruning

Since group-wise pruning can also be implemented via Skeleton, we perform group-wise pruning and SWP both based on the Skeleton. Figure 6 shows the results. We can see under the same number of parameters or Flops, SWP achieves a higher performance compared to group-wise pruning. We also find that in group-wise pruning, *layer2.7.conv1* and *layer2.7.conv2* will be identified as invalid (*i.e.*, all the weights in such layer will be pruned by the algorithm) when the pruning ratio reaches 76.64%. However, this phenomenon does not appear at stripe-wise pruning even with an 87.36% pruning ratio, which further verifies our hypothesis that group-wise pruning breaks the independent assumption on the filters and may easily lose representation ability. In contrast, SWP keeps each filter independent of each other, thus can achieve a higher pruning ratio.

4.3 Comparing SWP with state-of-art methods

We compare SWP with recent state-of-arts pruning methods. Table 2 and Table 3 lists the comparison on CIFAR-10 and ImageNet, respectively. In Table 2, IR [16] is group-wise pruning method, the others except SWP are filter-wise or channel-wise methods. We can see GBN [29] even outperforms the shape-wise pruning method. From our analysis, group-wise pruning regularizes the network’s weights in the same positions among all the filters, which may cause the network to lose useful information. Thus group-wise pruning may not be the best choice. However, SWP outperforms other methods by a large margin. For example, when pruning VGG16, SWP can reduce the number of parameters by 92.66% and the number of Flops by 71.16% without losing network performance. On ImageNet, SWP could also

¹<https://github.com/pytorch/examples/tree/master/imagenet>

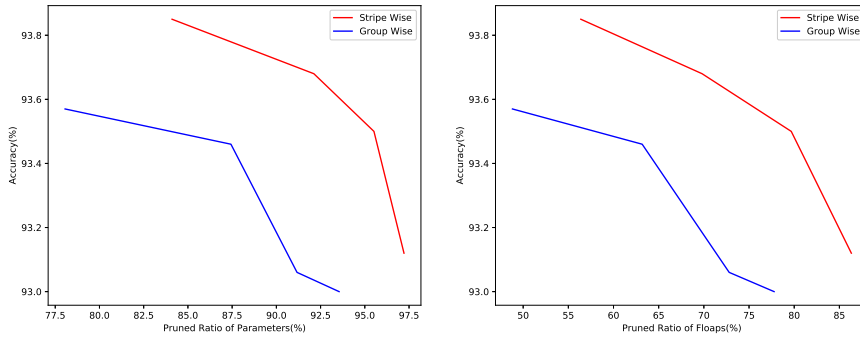


Figure 6: Comparing SWP with group-wise pruning on CIFAR-10. The backbone is VGG16.

Table 2: Comparing SWP with state-of-arts FP-based methods on CIFAR-10 dataset. The baseline accuracy of ResNet56 is 93.1% [29], while VGG16’s baseline accuracy is 93.25% [7].

Backbone	Metrics	Params(%)↓	FLOPS(%)↓	Accuracy(%)↓
VGG16	L1[7] (ICLR 2017)	64	34.3	-0.15
	ThiNet[24] (ICCV 2017)	63.95	64.02	2.49
	SSS[44] (ECCV 2018)	73.8	41.6	0.23
	SFP[45] (IJCAI 2018)	63.95	63.91	1.17
	GAL[27] (CVPR 2019)	77.6	39.6	1.22
	Hinge[46] (CVPR 2020)	80.05	39.07	-0.34
	HRank[47] (CVPR 2020)	82.9	53.5	-0.18
	Ours	92.66	71.16	-0.4
ResNet56	L1[7] (ICLR 2017)	13.7	27.6	-0.02
	CP[8] (ICCV 2017)	-	50	1.00
	NISP[25] (CVPR 2018)	42.6	43.6	0.03
	DCP[48] (NeurIPS 2018)	70.3	47.1	-0.01
	IR[16] (IJCNN 2019)	-	67.7	0.4
	C-SGD[49] (CVPR 2019)	-	60.8	-0.23
	GBN [29] (NeurIPS 2019)	66.7	70.3	0.03
	HRank[47] (CVPR 2020)	68.1	74.1	2.38
	Ours	77.7	75.6	0.12

Table 3: Comparing SWP with state-of-arts pruning methods on ImageNet dataset. All the methods use ResNet18 as the backbone and the baseline top-1 and top-5 accuracy are 69.76% and 89.08%, respectively.

Backbone	Metrics	FLOPS(%)↓	Top-1(%)↓	Top-5(%)↓
ResNet18	LCCL[50] (CVPR 2017)	35.57	3.43	2.14
	SFP[45] (IJCAI 2018)	42.72	2.66	1.3
	FPGM[51] (CVPR 2019)	42.72	1.35	0.6
	TAS[52] (NeurIPS 2019)	43.47	0.61	-0.11
	DMCP[53] (CVPR 2020)	42.81	0.56	-
	Ours ($\alpha = 5e - 6$)	50.48	-0.23	-0.22
	Ours ($\alpha = 2e - 5$)	54.58	0.17	0.04

achieve better performance than recent benchmark approaches. For example, SWP can reduce the FLOPs by 54.58% without an obvious accuracy drop. We want to emphasize that even though SWP brings indexes of strips, the cost is little. When performing calculation on the number of parameters, We have added these indexes in the calculation on Table 2 and Table 3. The pruning ratio of SWP is still significant and achieves state-of-art results.

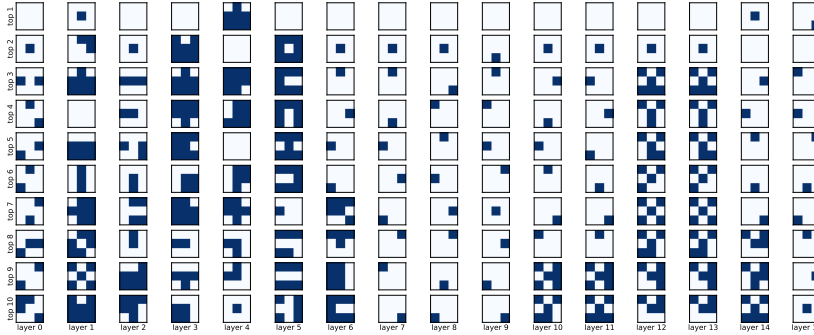


Figure 7: The visualization of the VGG19 filters pruned by SWP. From top to bottom, we display the filters according to their frequency in such layer. White color denotes the corresponding strip in the filter is removed by SWP.

Table 4: This table shows how α and δ affects SWP results. The experiment is conducted on CIFAR-10. The network is ResNet56.

α	0.8e-5	1.2e-5	1.4e-5	1e-5				
δ	0.05			0.01	0.03	0.05	0.07	0.09
Params (M)	0.25	0.21	0.2	0.45	0.34	0.21	0.16	0.12
Flops (M)	61.16	47.71	41.23	111.68	74.83	56.10	41.59	29.72
Accuracy(%)	92.73	92.43	92.12	93.25	92.82	92.98	92.43	91.83

4.4 Visualizing the pruned filters

We visualize the filters of VGG19 to show what the sparse network look like after pruning by SWP. The kernel size of VGG19 is $\mathbb{R}^{3 \times 3}$, thus there are 9 strips in each filter. Each filter has 2^9 forms since each strip can be removed or preserved. We display the filters of each layer according to their frequency of each form. Figure 7 shows the visualization results. There are some interesting phenomenons:

- For each layer, most filters are directly pruned with all the strips.
- In the middle layers, most preserved filters only have one strip. However, in the layers that close to input, most preserved layers have multiple strips. Suggesting the redundancy most happens in the middle layers.

We believe this visualization may towards a better understanding of CNNs. In the past, we always regard filter as the smallest unit in CNN. However, from our experiment, the architecture of the filter itself is also important and can be learned by pruning. More visualization results can be found in the supplementary material.

4.5 Ablation Study

In this section, we study how different hyper-parameters affect pruning results. We mainly study the weighting coefficient α in (1) and the pruning threshold δ . Table 4 shows the experimental results. We find $\alpha = 1e - 5$ and $\delta = 0.05$ gives the acceptable pruning ratio and test accuracy.

5 Conclusion

In this paper, we propose a new pruning paradigm called SWP. Instead of pruning the whole filter, SWP regards each filter as a combination of multiple stripes (*i.e.*, 1×1 filters), and performs pruning on the stripes. We also introduce Filter Skeleton (FS) to efficiently learn the optimal shape of the filters for pruning. Through extensive experiments and analyses, we demonstrate the effectiveness of the SWP framework. Future work can be done to develop a more efficient regularizer to further optimize DNNs.

Acknowledgements: The work was supported in part by the Shenzhen Fundamental Research Fund under Grant JCYJ20180306172023949, in part by the Guangdong Basic and Applied Basic Research Foundation under Grant 2019B1515120055, in part by the Shenzhen Research Institute of Big Data, in part by the Shenzhen Institute of Artificial Intelligence and Robotics for Society, and in part by the Medical Biometrics Perception and Analysis Engineering Laboratory, Shenzhen, China.

References

- [1] Alex Graves, Abdel-rahman Mohamed, and Geoffrey Hinton. Speech recognition with deep recurrent neural networks. In *2013 IEEE international conference on acoustics, speech and signal processing*, pages 6645–6649. IEEE, 2013.
- [2] Alex Krizhevsky, Ilya Sutskever, and Geoffrey E Hinton. Imagenet classification with deep convolutional neural networks. In *Advances in neural information processing systems*, pages 1097–1105, 2012.
- [3] William Lotter, Gabriel Kreiman, and David Cox. Deep predictive coding networks for video prediction and unsupervised learning. *arXiv preprint arXiv:1605.08104*, 2016.
- [4] Xiang Zhang and Yann LeCun. Text understanding from scratch. *arXiv preprint arXiv:1502.01710*, 2015.
- [5] Song Han, Jeff Pool, John Tran, and William Dally. Learning both weights and connections for efficient neural network. In *Advances in neural information processing systems*, pages 1135–1143, 2015.
- [6] Song Han, Huizi Mao, and William J Dally. Deep compression: Compressing deep neural networks with pruning, trained quantization and huffman coding. *arXiv preprint arXiv:1510.00149*, 2015.
- [7] Hao Li, Asim Kadav, Igor Durdanovic, Hanan Samet, and Hans Peter Graf. Pruning filters for efficient convnets. *arXiv preprint arXiv:1608.08710*, 2016.
- [8] Yihui He, Xiangyu Zhang, and Jian Sun. Channel pruning for accelerating very deep neural networks. In *Proceedings of the IEEE International Conference on Computer Vision*, pages 1389–1397, 2017.
- [9] Zhuang Liu, Jianguo Li, Zhiqiang Shen, Gao Huang, Shoumeng Yan, and Changshui Zhang. Learning efficient convolutional networks through network slimming. In *Proceedings of the IEEE International Conference on Computer Vision*, pages 2736–2744, 2017.
- [10] Zhuang Liu, Mingjie Sun, Tinghui Zhou, Gao Huang, and Trevor Darrell. Rethinking the value of network pruning. *arXiv preprint arXiv:1810.05270*, 2018.
- [11] Christian Szegedy, Wei Liu, Yangqing Jia, Pierre Sermanet, Scott Reed, Dragomir Anguelov, Dumitru Erhan, Vincent Vanhoucke, and Andrew Rabinovich. Going deeper with convolutions. In *The IEEE Conference on Computer Vision and Pattern Recognition (CVPR)*, June 2015.
- [12] Christian Szegedy, Vincent Vanhoucke, Sergey Ioffe, Jon Shlens, and Zbigniew Wojna. Rethinking the inception architecture for computer vision. In *Proceedings of the IEEE conference on computer vision and pattern recognition*, pages 2818–2826, 2016.
- [13] Xiaohan Ding, Yuchen Guo, Guiguang Ding, and Jungong Han. Acnet: Strengthening the kernel skeletons for powerful cnn via asymmetric convolution blocks. 2019.
- [14] Vadim Lebedev and Victor Lempitsky. Fast convnets using group-wise brain damage. In *Proceedings of the IEEE Conference on Computer Vision and Pattern Recognition*, pages 2554–2564, 2016.
- [15] Wei Wen, Chunpeng Wu, Yandan Wang, Yiran Chen, and Hai Li. Learning structured sparsity in deep neural networks. In *Advances in neural information processing systems*, pages 2074–2082, 2016.
- [16] Huan Wang, Qiming Zhang, Yuehai Wang, Lu Yu, and Haoji Hu. Structured pruning for efficient convnets via incremental regularization. In *2019 International Joint Conference on Neural Networks (IJCNN)*, pages 1–8. IEEE, 2019.
- [17] Yann LeCun, John S Denker, and Sara A Solla. Optimal brain damage. In *Advances in neural information processing systems*, pages 598–605, 1990.
- [18] Babak Hassibi and David G Stork. Second order derivatives for network pruning: Optimal brain surgeon. In *Advances in neural information processing systems*, pages 164–171, 1993.
- [19] Yiwen Guo, Anbang Yao, and Yurong Chen. Dynamic network surgery for efficient dnns. In *Advances in neural information processing systems*, pages 1379–1387, 2016.
- [20] Alireza Aghasi, Afshin Abdi, Nam Nguyen, and Justin Romberg. Net-trim: Convex pruning of deep neural networks with performance guarantee. In *Advances in Neural Information Processing Systems*, pages 3177–3186, 2017.
- [21] Zhenhua Liu, Jizheng Xu, Xiulian Peng, and Ruiqin Xiong. Frequency-domain dynamic pruning for convolutional neural networks. In *Advances in Neural Information Processing Systems*, pages 1043–1053, 2018.
- [22] Hyeong-Ju Kang. Accelerator-aware pruning for convolutional neural networks. *CoRR*, abs/1804.09862, 2018.
- [23] Song Han, Xingyu Liu, Huizi Mao, Jing Pu, Ardavan Pedram, Mark A Horowitz, and William J Dally. Eie: efficient inference engine on compressed deep neural network. *ACM SIGARCH Computer Architecture News*, 44(3):243–254, 2016.

- [24] Jian-Hao Luo, Jianxin Wu, and Weiyao Lin. Thinet: A filter level pruning method for deep neural network compression. In *Proceedings of the IEEE international conference on computer vision*, pages 5058–5066, 2017.
- [25] Ruichi Yu, Ang Li, Chun-Fu Chen, Jui-Hsin Lai, Vlad I Morariu, Xintong Han, Mingfei Gao, Ching-Yung Lin, and Larry S Davis. Nisp: Pruning networks using neuron importance score propagation. In *Proceedings of the IEEE Conference on Computer Vision and Pattern Recognition*, pages 9194–9203, 2018.
- [26] Yihui He, Ji Lin, Zhijian Liu, Hanrui Wang, Li-Jia Li, and Song Han. Amc: Automl for model compression and acceleration on mobile devices. In *Proceedings of the European Conference on Computer Vision (ECCV)*, pages 784–800, 2018.
- [27] Shaohui Lin, Rongrong Ji, Chenqian Yan, Baochang Zhang, Liujuan Cao, Qixiang Ye, Feiyue Huang, and David Doermann. Towards optimal structured cnn pruning via generative adversarial learning. In *Proceedings of the IEEE Conference on Computer Vision and Pattern Recognition*, pages 2790–2799, 2019.
- [28] Carl Lemaire, Andrew Achkar, and Pierre-Marc Jodoin. Structured pruning of neural networks with budget-aware regularization. In *Proceedings of the IEEE Conference on Computer Vision and Pattern Recognition*, pages 9108–9116, 2019.
- [29] Zhonghui You, Kun Yan, Jinmian Ye, Meng Ma, and Ping Wang. Gate decorator: Global filter pruning method for accelerating deep convolutional neural networks. In *Advances in Neural Information Processing Systems*, pages 2130–2141, 2019.
- [30] Jonathan Frankle and Michael Carbin. The lottery ticket hypothesis: Finding sparse, trainable neural networks. *arXiv preprint arXiv:1803.03635*, 2018.
- [31] Huizi Mao, Song Han, Jeff Pool, Wenshuo Li, Xingyu Liu, Yu Wang, and William J Dally. Exploring the granularity of sparsity in convolutional neural networks. In *Proceedings of the IEEE Conference on Computer Vision and Pattern Recognition Workshops*, pages 13–20, 2017.
- [32] Zehao Huang and Naiyan Wang. Data-driven sparse structure selection for deep neural networks. *ECCV*, 2018.
- [33] Aditya Kusupati, Vivek Ramanujan, Raghav Somani, Mitchell Wortsman, Prateek Jain, Sham Kakade, and Ali Farhadi. Soft threshold weight reparameterization for learnable sparsity. In *Proceedings of the International Conference on Machine Learning*, July 2020.
- [34] Aditya Kusupati, V. Ramanujan, Raghav Somani, Mitchell Wortsman, Prateek Jain, Sham M. Kakade, and Ali Farhadi. Soft threshold weight reparameterization for learnable sparsity. *ArXiv*, abs/2002.03231, 2020.
- [35] Kai Han, Yunhe Wang, Yixing Xu, Chunjing Xu, Dacheng Tao, and Chang Xu. Full-stack filters to build minimum viable cnns. *arXiv preprint arXiv:1908.02023*, 2019.
- [36] Ting Wu Chin, Ruizhou Ding, Cha Zhang, and Diana Marculescu. Towards efficient model compression via learned global ranking. *arXiv*, 2019.
- [37] Carl Lemaire, Andrew Achkar, and Pierre Marc Jodoin. Structured pruning of neural networks with budget-aware regularization. 2018.
- [38] Bichen Wu, Alvin Wan, Xiangyu Yue, Peter Jin, Sicheng Zhao, Noah Golmant, Amir Gholaminejad, Joseph Gonzalez, and Kurt Keutzer. Shift: A zero flop, zero parameter alternative to spatial convolutions. 2017.
- [39] Yao Lu, G. Lu, Bob Zhang, Yuanrong Xu, and Jinxing Li. Super sparse convolutional neural networks. In *AAAI*, 2019.
- [40] Alex Krizhevsky, Geoffrey Hinton, et al. Learning multiple layers of features from tiny images. 2009.
- [41] Jia Deng, Wei Dong, Richard Socher, Li-Jia Li, Kai Li, and Li Fei-Fei. Imagenet: A large-scale hierarchical image database. In *2009 IEEE conference on computer vision and pattern recognition*, pages 248–255. Ieee, 2009.
- [42] Karen Simonyan and Andrew Zisserman. Very deep convolutional networks for large-scale image recognition. *arXiv preprint arXiv:1409.1556*, 2014.
- [43] Kaiming He, Xiangyu Zhang, Shaoqing Ren, and Jian Sun. Deep residual learning for image recognition. In *Proceedings of the IEEE conference on computer vision and pattern recognition*, pages 770–778, 2016.
- [44] Zehao Huang and Naiyan Wang. Data-driven sparse structure selection for deep neural networks. In *Proceedings of the European conference on computer vision (ECCV)*, pages 304–320, 2018.
- [45] Yang He, Guoliang Kang, Xuanyi Dong, Yanwei Fu, and Yi Yang. Soft filter pruning for accelerating deep convolutional neural networks. *arXiv preprint arXiv:1808.06866*, 2018.
- [46] Yawei Li, Shuhang Gu, Christoph Mayer, Luc Van Gool, and Radu Timofte. Group sparsity: The hinge between filter pruning and decomposition for network compression. *arXiv preprint arXiv:2003.08935*, 2020.
- [47] Mingbao Lin, Rongrong Ji, Yan Wang, Yichen Zhang, Baochang Zhang, Yonghong Tian, and Ling Shao. Hrank: Filter pruning using high-rank feature map. *arXiv preprint arXiv:2002.10179*, 2020.
- [48] Zhuangwei Zhuang, Mingkui Tan, Bohan Zhuang, Jing Liu, Yong Guo, Qingyao Wu, Junzhou Huang, and Jinhui Zhu. Discrimination-aware channel pruning for deep neural networks. In *Advances in Neural Information Processing Systems*, pages 875–886, 2018.
- [49] Xiaohan Ding, Guiguang Ding, Yuchen Guo, and Jungong Han. Centripetal sgd for pruning very deep convolutional networks with complicated structure. In *Proceedings of the IEEE Conference on Computer Vision and Pattern Recognition*, pages 4943–4953, 2019.

- [50] Xuanyi Dong, Junshi Huang, Yi Yang, and Shuicheng Yan. More is less: A more complicated network with less inference complexity. In *Proceedings of the IEEE Conference on Computer Vision and Pattern Recognition*, pages 5840–5848, 2017.
- [51] Yang He, Ping Liu, Ziwei Wang, Zhilan Hu, and Yi Yang. Filter pruning via geometric median for deep convolutional neural networks acceleration. In *Proceedings of the IEEE Conference on Computer Vision and Pattern Recognition*, pages 4340–4349, 2019.
- [52] Xuanyi Dong and Yi Yang. Network pruning via transformable architecture search. In *Advances in Neural Information Processing Systems*, pages 759–770, 2019.
- [53] Shaopeng Guo, Yujie Wang, Quanquan Li, and Junjie Yan. Dmcp: Differentiable markov channel pruning for neural networks. *arXiv preprint arXiv:2005.03354*, 2020.

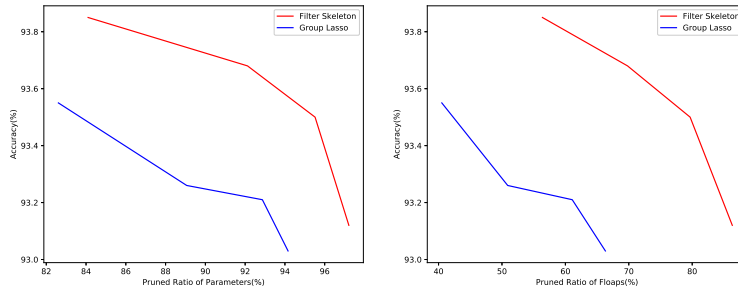


Figure 8: Comparing Filter Skeleton with Lasso regularizer on CIFAR-10. The backbone is VGG16.

6 Supplementary Material

This is the supplementary material for the paper ‘Pruning Filter in Filter’. Section 6.1 shows that we can use SWP to continue pruning the network pruned by other FP (filter pruning) based methods. Section 6.2 shows that Filter Skeleton is better than lasso regularization in the SWP framework. Section 6.3 displays more visualization results.

6.1 Continual Pruning in SWP

Since SWP can achieve finer granularity than traditional filter pruning methods, we can use SWP to continue pruning the network pruned by other methods without obvious accuracy drop. Table 5 shows the experimental results. It can be observed that SWP can help other FP-based pruning towards higher pruning ratios.

Table 5: This table shows variant pruning methods on CIFAR-10 dataset. $A + B$ denotes that first prune the network with method A, then continue pruning the network with method B.

Backbone	Metrics	FLOPS (M)	Params (M)	Accuracy
VGG16	Baseline	14.72	627.36	93.63
	Network Slimming [9]	1.44	272.83	93.60
	Network Slimming + SWP	1.09	204.02	93.62
VGG19	Baseline	20.04	797.61	93.92
	DCP[48]	10.36	398.42	93.6
	DCP+SWP	3.40	253.24	93.4
ResNet56	Baseline	0.86	251.49	93.1
	GBN [29]	0.30	112.77	92.89
	GBN+SWP	0.24	81.26	92.67

6.2 Filter Skeleton v.s. Group Lasso

In the paper, we use Filter Skeleton (FS) to learn the optimal shape of each filter and prune the unimportant stripes. However, there exist other techniques to regularize the network to make it sparse. For example, Lasso-based regularizer [15], which directly regularizes the network weights. We offer a comparison to Group Lasso regularizer in this section. Figure 8 shows the results. We can see under the same number of parameters or Flops, PFF with Filter Skeleton achieves a higher performance.

6.3 More Visualization Results

In this section, we show how the pruned network look like by SWP. Figure 9 shows the visualization results of ResNet56 on CIFAR-10. It can be observed that (1) SWP has a higher pruning ratio on the middle layers, *e.g.*, layer 2.3 to layer 2.9. (2) The pruning ratio of each stripe is different and varies on each layer. Table 6 shows the pruned network on ImageNet. For example, in layer1.1.conv2, there are original 64 filters whose size is $\mathbb{R}^{62 \times 3 \times 3}$. After pruning, there exists 300 stripes whose size is $\mathbb{R}^{62 \times 1 \times 1}$. The pruning ratio in this layer is $1 - \frac{300 \times 62 \times 1 \times 1}{64 \times 62 \times 3 \times 3} = 0.47$.

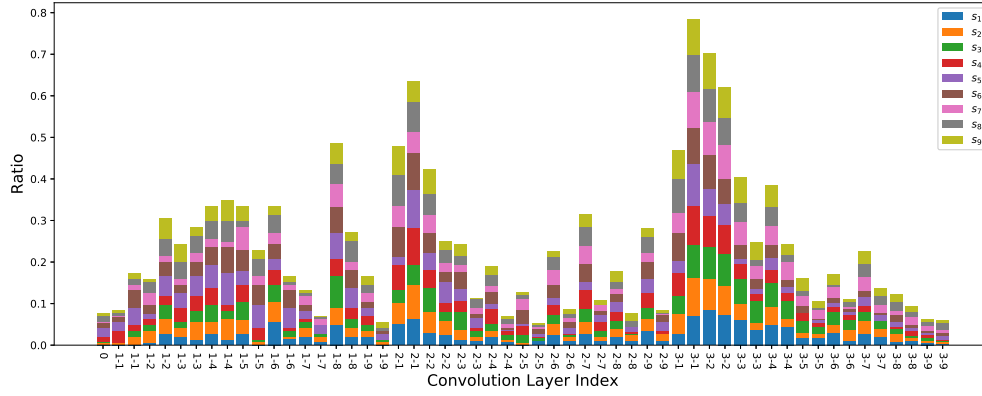


Figure 9: In the figure, We exhibit the ratio of remaining stripes of each layer. Each filter has 9 stripes indexed from s_1 to s_9 .

Table 6: This table shows the structure of pruned ResNet18 on ImageNet.

keys	modules
(conv1):	Strip(3,324)
(bn1):	BatchNorm(64)
(layer1.0.conv1):	Strip(64,102)
(layer1.0.bn1):	BatchNorm(57)
(layer1.0.conv2):	Strip(57,164)
(layer1.0.bn2):	BatchNorm(64)
(layer1.1.conv1):	Strip(64,175)
(layer1.1.bn1):	BatchNorm(62)
(layer1.1.conv2):	Strip(62,300)
(layer1.1.bn2):	BatchNorm(64)
(layer2.0.conv1):	Strip(64,475, stride=2)
(layer2.0.bn1):	BatchNorm(119)
(layer2.0.conv2):	Strip(119,636)
(layer2.0.bn2):	BatchNorm(128)
(layer2.1.conv1):	Strip(128,662)
(layer2.1.bn1):	BatchNorm(128)
(layer2.1.conv2):	Strip(128,648)
(layer2.1.bn2):	BatchNorm(128)
(layer3.0.conv1):	Strip(128,995, stride=2)
(layer3.0.bn1):	BatchNorm(252)
(layer3.0.conv2):	Strip(252,1502)
(layer3.0.bn2):	BatchNorm(256)
(layer3.1.conv1):	Strip(256,1148)
(layer3.1.bn1):	BatchNorm(256)
(layer3.1.conv2):	Strip(256,944)
(layer3.1.bn2):	BatchNorm(256)
(layer4.0.conv1):	Strip(256,1304, stride=2)
(layer4.0.bn1):	BatchNorm(498)
(layer4.0.conv2):	Strip(498, 2448)
(layer4.0.bn2):	BatchNorm(512)
(layer4.1.conv1):	Strip(512, 3111)
(layer4.1.bn1):	BatchNorm(512)
(layer4.1.conv2):	Strip(512, 2927)
(layer4.1.bn2):	BatchNorm(512)
(fc):	Linear(512,1000)